Low Power Consumption Multimode Laser Diode Module for 900-nm Band (915~975 nm)

*by Naoki Hayamizu *, Jun Miyokawa *, Yuichiro Irie *, Shuichi Tanaka *, Yasuo Oeda *2, Tsuyoshi Fujimoto *2 and Yoshikazu Ikegami *2*

ABSTRACT A low power consumption multimode laser diode module (MM-LDM) for the 900-nm band (915~975 nm) has been developed for use in material processing and measurement systems.

This LDM has advantages over conventional modules in terms of higher power, smaller size and lower power consumption. In this paper, we report how improvement of the characteristics of the 900-nm band MM-LDM with a standard 14-pin butterfly package was achieved by increasing the power conversion efficiency of the laser diode chip and the optical coupling efficiency with multimode fiber, and by optimizing heat dissipation design.

1. INTRODUCTION

Gas lasers like CO_2, Ar or excimer lasers, and solid-state lasers like YAG lasers pumped by lamps have been used widely in industrial fields including material processing (cutting, welding, soldering and marking) or measurement systems. These lasers, however, had some disadvantages in terms of large power consumption, frequent maintenance and short lifetime. Recently, high power laser diodes have been attracting attention because they have the advantages of smaller size, higher electrical-to-optical conversion efficiency, higher reliability and superior productivity, and they have begun to be used for direct processing and as the pumping light for solid-state lasers. Especially, cladding pump fiber lasers pumped by light from laser diodes is rapidly coming into widespread use because it has a higher beam quality than gas or solid-state lasers. High-power 808-nm laser diodes are being used for medical appliances and printing devices. In telecommunications, high-power 900-nm band laser diodes are used in cladding pump amplifiers for CATV. High-power 900-nm and 808-nm band multimode laser diode modules (MM-LDMs) are becoming important in various applications, but since they were developed focusing on high output power only, they have the following problems:

1) large power consumption owing to un-optimized heat dissipation design;
2) incompatibility owing to the large packages and package dimension that differ vendor by vendor; and
3) inconvenience owing to an output optical interface without using an optical fiber.

The large and incompatible packages complicate the design of circuit board heat dissipation, and large power consumption makes it difficult to downsize the package and reduce running cost.

In this paper, we report approaches that we adopted in order to develop a 900-nm band MM-LDM with high power and low power consumption, namely:

1) using a high-power laser diode chip with high conversion efficiency;
2) improving coupling efficiency to the optical fiber;
3) improving the heat dissipation of the module; and
4) using a standard 14-pin butterfly package.

2. LASER DIODES

2.1 Laser Diode Design [1)]

The 900-nm band multimode laser diode (MM-LD) is being produced by MC-FITEL, a joint venture between Furukawa Electric and Mitsui Chemicals.

The MM-LD consists of InGaAs/AlGaAs material that is epitaxitially grown by low-pressure metalorganic chemical vapor deposition (MOCVD). Figure 1 shows a cross-sectional view. Stripe width was controlled to 100 μm by an n-GaAs current blocking layer buried in a p-type GaAs cap layer. The front facet had a low-reflectivity coating (4 %) and the rear facet a high-reflectivity coating (96 %). The cavity length was 1.8 mm. This MM-LD features adoption of a decoupled confinement heterostructure (DCH), achieving both higher power and higher efficiency.

* Semiconductor Device Development Dept., R&D Div.
*2 MC-FITEL Inc.

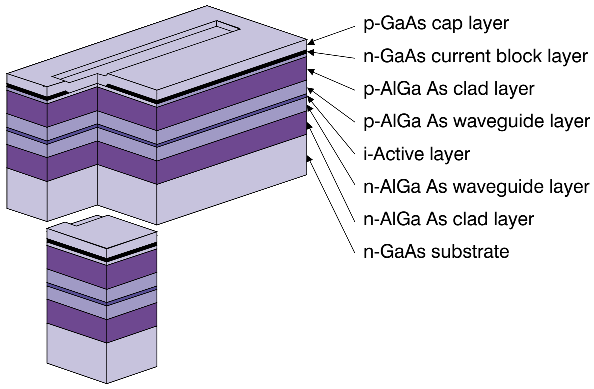

Figure 1 Cross-sectional view of MM-LD chip.

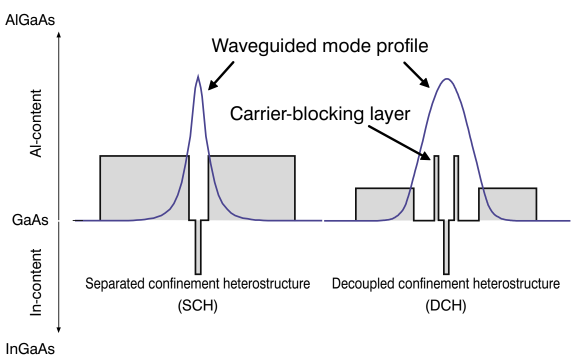

Figure 2 Comparison of the separate-confinement and decoupled confinement heterostructures.

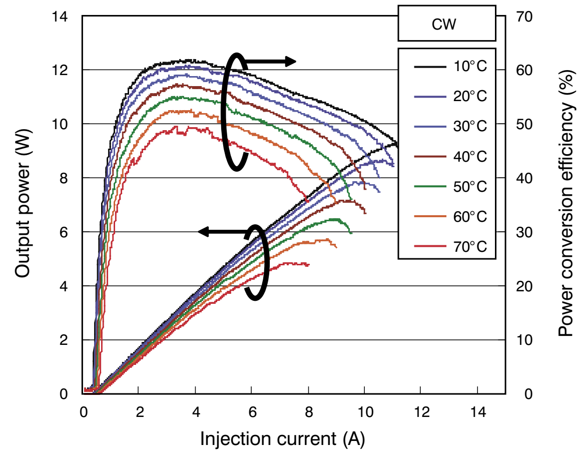

Figure 3 *LI* characteristics of typical LD chip.

2.1.1 Decoupled Confinement Heterostructure [2)]

The separated confinement heterostructure (SCH) with a single quantum well is a popular structure in high-power InGaAs/AlGaAs LDs, but makes it difficult to confine the carrier completely in a narrow active region. The waveguide layer is thus narrower and therefore must be made deeper in energy level than the clad layer. The design of the waveguided mode is limited by the relation between the bandgap and the refraction index in InGaAs/AlGaAs LDs.

On the other hand, the DCH confines carriers in the active region by wide bandgap carrier-blocking layers located at both sides of the quantum well, making it possible to design the waveguide structure independently of the carrier confinement structure.

2.1.2 Improvement of COD Level [2)]

The maximum power of an InGaAs/AlGaAs LD is generally limited by the incidence of catastrophic optical damage (COD), which may be caused by re-coupling of carriers, oxidation of the facet, or increased temperature due to absorption of emitted light at the facet. Decreasing the optical density at the facet is an effective way to limit the incidence of COD, and the DCH decreases the optical density at the facet to improve the waveguided mode profile as shown Figure 2. Moreover, we have improved the incident level of COD by setting up a non-current injection layer near the front facet of the LD.

2.1.3 Reduction of Thermal and Electrical Resistance [2)]

In addition to COD, saturation of optical output power as LD temperature increases is also a major factor limiting output power. To prevent the increase in LD temperature, it is useful to use materials of low electrical resistance, and to suppress generation of Joule's heat and ensure thermal conductivity the use of material of low thermal resistance is indicated. In InGaAs/AlGaAs lasers, low thermal and electrical resistance can be realized by reducing the Al content of the clad layers. The conventional SCH cannot block the overflow of carriers since reducing the Al content of the clad layers induces a decrease in bandgap energy at the clad layer.

DCH lasers can realize low thermal and electrical resistance without carrier overflow since the waveguide structure can be designed independently of the carrier confinement structure.

2.2 LD Chip Characteristics [1)]

2.2.1 Optical Output Power

Figure 3 shows the *LI* characteristic of a typical 900-nm band MM-LD chip at selected temperatures. LD chips with a cavity length of 1.8 mm and DCH achieved high power and high conversion efficiency at the same time, with a maximum output power of 9 W and a power conversion efficiency of 62 %.

2.2.2 Far-Field Pattern

Figure 4 shows the far-field pattern (FFP) of a typical MM-LD. In the vertical direction the beam intensity distribution for the active region was almost Gaussian, but in the horizontal direction was substantially rectangular.

The vertical beam divergence angle was 33 deg. for full width at half maximum (FWHM) and 70 deg. for $1/e^2$. The horizontal beam divergence was about 10 deg, smaller than the numerical aperture (NA) =0.1 up to 4 W. The horizontal beam divergence increased slightly with optical power because of the thermal lens effect.

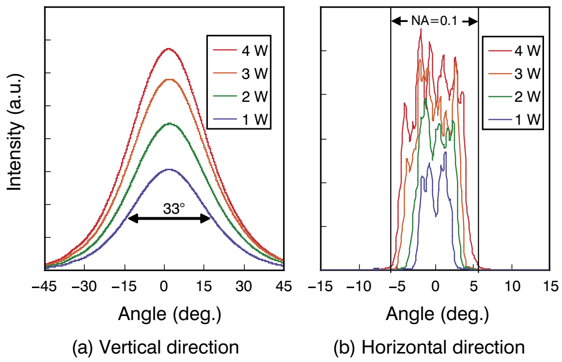

Figure 4 FFP of a typical MM-LD chip.

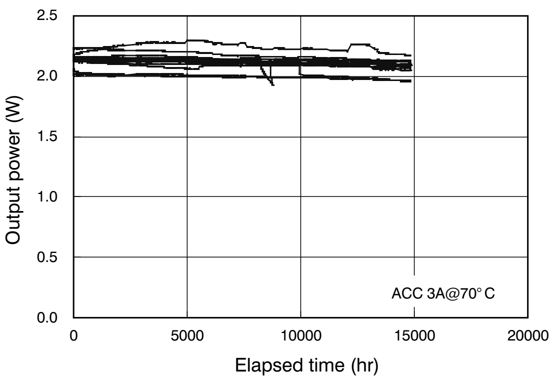

Figure 5 Results of accelerated aging test of MM-LD chips.

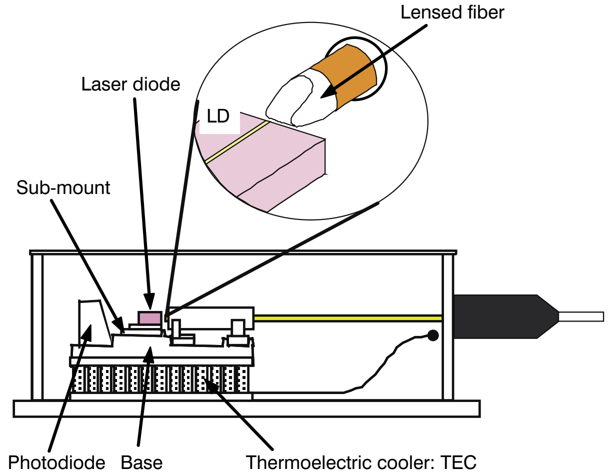

Figure 6 Cross-sectional view of MM-LDM.

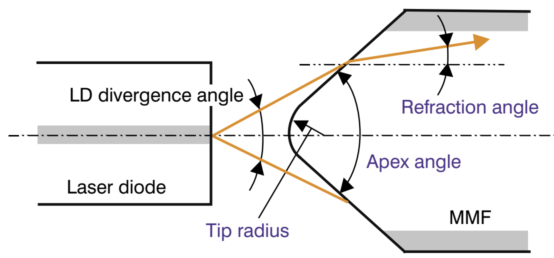

Figure 7 Configuration of optical coupling between LD chip and lensed fiber.

2.2.3 Reliability

Accelerated aging test of LDs was carried out at 70°C under auto current control (ACC) of 3 A for 15,000 hours (see Figure 5). At a fiber output power of 1.5 W at 25°C, the random failure rate can be estimated at 490 FIT and the median lifetime at 1,400,000 hours.

3. LASER DIODE MODULE DESIGN

To realize a laser diode module with high power and low power consumption, it is important to have high LD-to-fiber coupling efficiency, stable structure and efficient heat dissipation design.

3.1 Basic Design

Design of the multimode laser diode module (MM-LDM) follows that of the 980-nm single-mode laser diode module (SM-LDM). Figure 6 shows a cross-sectional view of an MM-LDM. The LD chip was bonded on a CuW sub-mount in a junction-down configuration. The sub-mount was fixed to a base on which a multi-mode fiber (MMF) and a photodiode (PD) for power monitoring were also mounted. The optical lensed fiber has a micro lens at the tip of the MMF, and is fixed by YAG welding. LD temperature is kept constant by a thermoelectric cooler (TEC) fixed under the base.

3.2 Improving Coupling Efficiency [3)]

The design of the lensed fiber is important in achieving high optical coupling efficiency. The shape of the lensed fiber was arrived at by taking account of the FFP of the typical MM-LD shown in Figure 4. We considered the vertical and horizontal components of the beam separately since the shape of the beam emitted from the LD was elliptical. In the horizontal component, the optical coupling is thought to be butt coupling. As described in Section 2.2.2, the horizontal beam divergence was smaller than NA=0.1, which is smaller than that of the MMF, and the core diameter of the MMF, at 105 μm, was substantially equal to the stripe width of the LD, which was 100 μm. Thus the horizontal component of LD-to-MMF coupling is not critical, because our MMF had an NA of 0.15.

We designed the lens shape assuming that the wedge consisted of two parts: one an inclined plane and the other was a spherical part located at the tip of the wedge. Lens shape could thus be described by apex angle and tip radius. Figure 7 shows the optical coupling configuration between the LD chip and the lensed fiber. The lens was formed at the tip of the optical fiber where the core diameter was 105 μm. Because the focus length was short and the lensed fiber was close enough to the LD facet, the apex angle and the tip radius were designed on the following two assumptions:

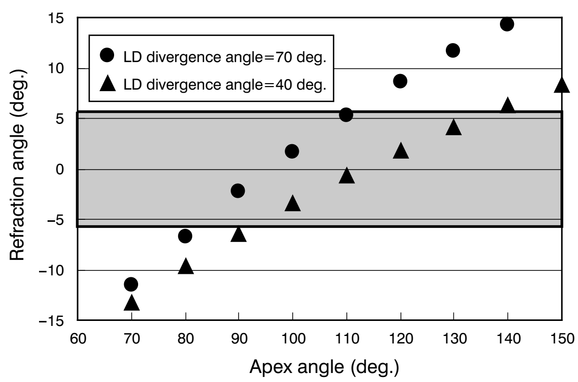

Figure 8 Apex angle dependence of refraction angle for incident light of 70 deg. and 40 deg.

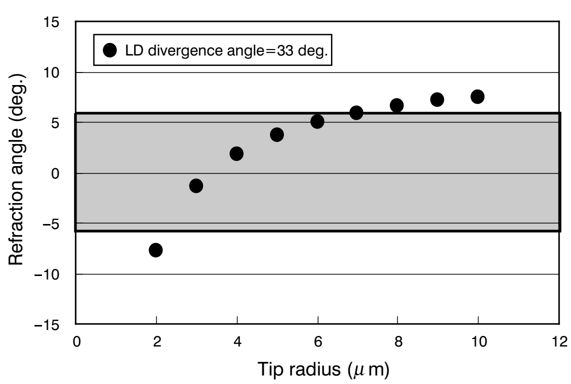

Figure 9 Tip radius dependence of refraction angle for incident light of FWHM.

1) emitted light with an FFP narrower than the FWHM is coupled to the optical fiber through the spherical part; and
2) emitted light with a wide divergence angle between the FWHM and $1/e^2$ is coupled to the optical fiber through the inclined plane.

When we design the apex angle, the apex angle needs to be considered only for $1/e^2$, which is 70 deg. of LD divergence angle, to obtain high coupling efficiency. Figure 8 shows the apex angle dependence of the refraction angle for incident light with divergence angles of 70 deg. and 40 deg. respectively. MMF of NA=0.15 can propagate light when the refraction angle falls within the gray area. In this result, we could select apex angles from 90 to 110 deg. for a 70-deg. divergence angle, and for a 40-deg. divergence angle, the apex angle could be from 90 to 130 deg. An apex angle of 110 deg. is therefore thought to be the optimum angle for coupling light with the optical fiber at divergence angles between FWHM and $1/e^2$ through the inclined plane.

Figure 9 shows the tip radius dependence of the refraction angle for incident light with FWHM divergence angle. In this result, a tip radius from 2.5 to 7 μm can be selected. The actual apex angle was determined as 5 μm taking account of reproducibility and ease of processing of the tip radius.

In prototype production, we obtained a maximum coupling efficiency of 90 % and an average of 87 %.

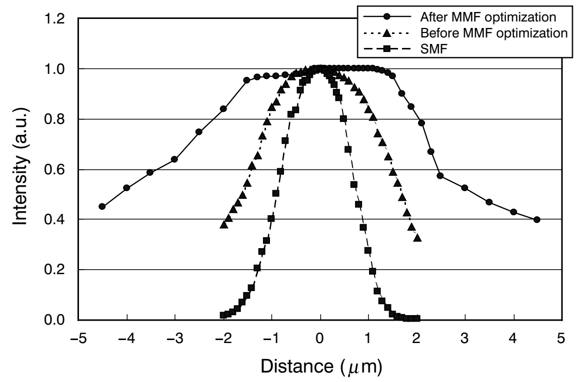

Figure 10 Comparison of coupling tolerances between MM and SM lensed fibers.

An investigation of coupling tolerances for a lensed fiber of optimum design was carried out, and Figure 10 shows a comparison of coupling tolerances for MM and SM lensed fibers in the vertical direction of the LD. The SM lensed fiber coupling tolerance was extremely narrow (1 μm) since the mode field diameter of the SMF for 980 nm was only 6 μm. The MM lensed fiber had a wider coupling tolerance than the SM fiber even without optimization of its lens shape, since the core diameter of the MMF is so large (105 μm). However, we obtained a flat tolerance level of 4 μm to optimize the shape of the lensed fiber according to the studies mentioned above.

The coupling efficiency of the SM lensed fiber decreased 10 % only by the lensed fiber moving approximately 0.3 μm. Our 980-nm SM-LDM suppresses this decrease in coupling efficiency by precise YAG welding technique. The MM-LDM, having the same module structure and wide coupling tolerance, does not show any decrease in coupling efficiency with changes in ambient temperature or long-term usage. Moreover, since the MM-LDM has a high coupling tolerance, production is very easy and a high yield can be expected.

3.3 Heat Dissipation Design

To improve the heat dissipation characteristics of the module, it is desirable to increase the thermal conductivity of the structural materials from the LD to immediately above the TEC and to use a TEC having highly endothermic characteristics. Attention must be paid, however, to the decrease in coupling efficiency caused by changes in ambient temperature and to long-term reliability, which is a function of difference in the thermal expansion coefficients among the structural materials used in the module. The total power consumption of the module will also increase when we use a TEC with unnecessarily large endothermic characteristics.

We optimized thermal conductivity and thermal expansion coefficients among the materials used in the module. In addition, heat conduction for the MM-LDM is improved by using a large sub-mount which can dissipate the heat effectively. Figure 11 shows the LD injection

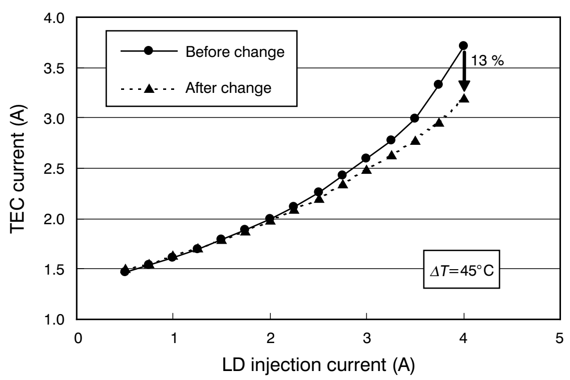

Figure 11 LD injection current dependence of TEC current.

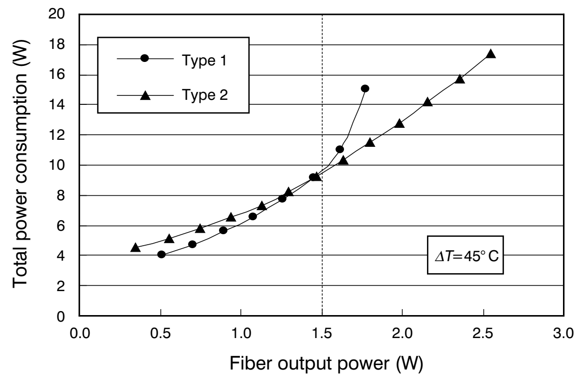

Figure 13 Comparison of total power consumption of two types of TEC.

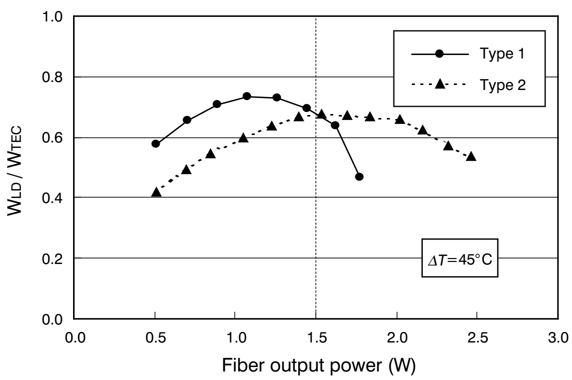

Figure 12 Comparison of efficiency of two types of TEC.

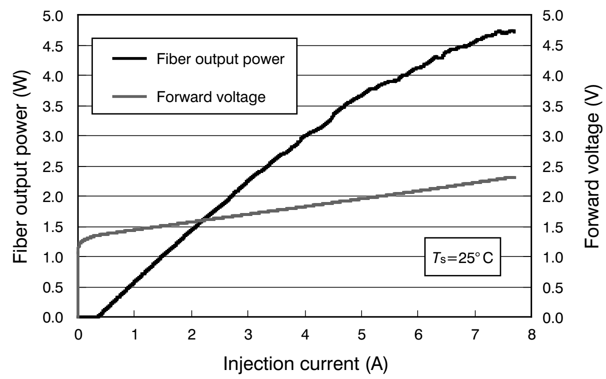

Figure 14 *LI* characteristics of typical MM-LDM.

current dependence of TEC current. It was reduced by 13 % at 4 A of LD current by optimizing the heat dissipation design.

To achieve lower power consumption, we have to select the best TEC by considering the operating region in which it dissipates heat from the LD most effectively. Figure 12 shows a comparison of the efficiency of two types of TEC. TEC efficiency is defined by W_{LD}/W_{TEC}, which shows the ratio of dissipated heat to the total power consumption of the TEC. The value of W_{LD}/W_{TEC} means efficient thermal transfer. The Type 1 TEC has an endothermic quantity Q_C of 2.4 W at a temperature difference (ΔT) between the hot and cold side of the TEC of 45°C, which is obtained from an LD temperature of 25 °C and an ambient temperature of 70°C. The Type 1 TEC is comparatively more efficient when dissipating a small quantity of heat. The Type 2 TEC has a Q_C of 3.0 W at a ΔT of 45°C, and is comparatively more efficient when dissipating a large quantity of heat.

As shown in Figure 12, Type 1 shows higher efficiency at fiber outputs below 1.5 W, while Type 2 efficiency is higher at outputs above that value. Figure 13 compares the total actual power consumption of modules using the two TECs, calculated by adding the values for the LD and the TEC. Total power consumption using the Type 1 TEC was lower at fiber outputs below 1.5 W, and that using the Type 2 TEC was lower at outputs above that value.

Accordingly it was decided to use the Type 1 TEC at fiber outputs power below 1.5 W and the Type 2 in the region above 1.5 W for MM-LDM under an ambient temperature of 70°C and an LD temperature of 25°C. We have also been able to propose an MM-LDM that has lower total power consumption for each customer's specification.

4. CHARACTERISTICS OF LASER DIODE MODULE

4.1 Fiber Output Power

Figure 14 shows the *LI* characteristics of a typical MM-LDM at an LD temperature of 25°C under continuous-wave (CW) operation. The threshold current was 344 mA and the slope efficiency was 0.9 W/A at the maximum. The maximum fiber output power was 4.7 W at an injection current of 7.7 A, but we regulated the fiber output power down to 2.5 W for production from the viewpoint of overall LDM reliability. The injection current was 3.35 A and the forward voltage was 1.74 V at a fiber output power of 2.5 W.

4.2 Optical Output Spectrum

Figure 15 shows a typical optical output spectrum of a 975-nm MM-LDM. We have been able to produce an MM-LDM with a wavelength tolerance of ±3 nm. The spectrum width was approximately 3 nm.

The output power dependence of the wavelength shift coefficient was 1.3 nm/W. This wavelength shift was

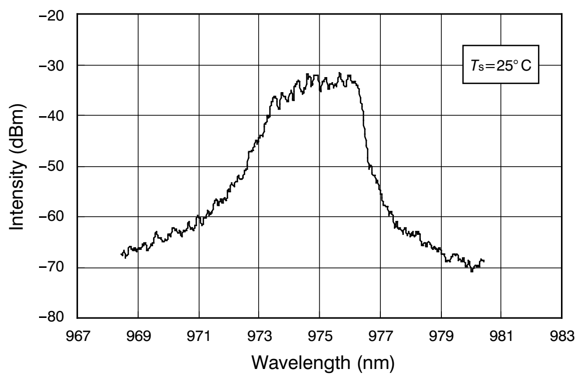

Figure 15 Typical optical output spectrum of MM-LDM.

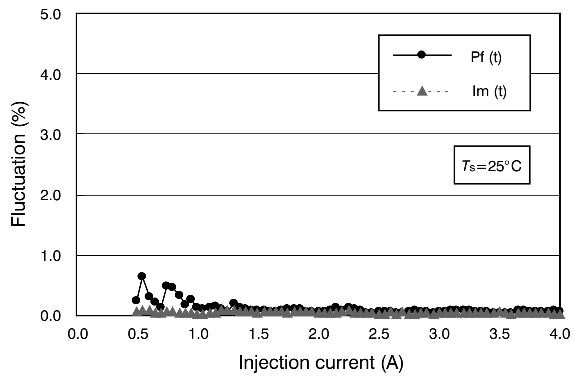

Figure 16 Time stability of fiber output power and monitor current.

induced by raising the temperature of the active region by supplying electric power to the LD. The wavelength shift can be controlled by TEC temperature changing since the LD temperature dependence of the wavelength shift coefficient was 0.35 nm/°C.

4.3 Total Power Consumption

As shown in Figure 13, the total power consumption was 9.3 W at a fiber output power of 1.5 W and 17.4 W at a fiber output power of 2.5 W using the Type 2 TEC. This total power consumption is 30 % lower than that of a conventional module with the butterfly package.

4.4 Time Stability of Fiber Output Power and Monitor Current

Figure 16 shows the injection current dependence of the time stability of fiber output power and monitor current. The time stability was excellent, with a fluctuation of less than 1 % over injection currents ranging from 0.5 to 4 A. This suggests that this MM-LDM can be utilized as the pump source of cladding optical amplifiers for CATV.

5. CONCLUSION

We have developed a multimode laser diode module for the 900-nm band for use as the pumping light source for fiber and the solid-state lasers, not only in the telecom field but also in certain industrial fields. We achieved a multimode laser diode module with 14-pin butterfly package that has a total power consumption approximately 30 % lower than that of conventional LDMs. Moreover, our MM-LDM can be used for optical amplifiers in the telecom field since it exhibits excellent time stability.

REFERENCES

1) Y. Oeda, F. Fujimoto: OAA'02 (2002), OMB1-1
2) K. Muro et al.: Functional Materials, August, 1997 (in Japanese)
3) K. Kono: Fundamentals and Applications of Optics Systems for Optical Devices, Gendai Kogaku Publisher, (in Japanese)
4) N. Hayamizu, J. Miyokawa, H. Murata, K. Nishikata, Y. Oeda, T. Fujimoto, Y. Ikegami : OAA'03 (2003), TuB4